Alpha-mangostin dephosphorylates ERM to induce adhesion and decrease surface stiffness in KG-1 cells

Thi Kieu Trang Phan[1,2,†], Thi Ly Do[1,†], Kouichi Tachibana[3,4], Takanori Kihara[1,*]

[1] Department of Life and Environment Engineering, Faculty of Environmental Engineering, The University of Kitakyushu, 1-1 Hibikino, Wakamatsu, Kitakyushu, Fukuoka 808-0135, Japan
[2] Vinmec Research Institute of Stem Cell and Gene Technology, Vinmec Health Care System, 458 Minh Khai, Hai Ba Trung, Hanoi, Vietnam
[3] Biomedical Research Institute, National Institute of Advanced Industrial Science and Technology (AIST), 1-1-1 Higashi, Tsukuba, Ibaraki 305-8566, Japan
[4] Department of Hematology and Oncology, Tokai University School of Medicine, 143 Shimokasuya, Isehara, Kanagawa, 259-1193, Japan

[†] These authors contributed equally.
[*] Corresponding author. Tel: +81-93-695-3290
E-mail address: tkihara@kitakyu-u.ac.jp (T. Kihara)

Acknowledgments
This work was partly conducted at the Instrumentation Center, The University of Kitakyushu.

Author contributions
TKTP, KT, and TK conceived and designed the work. TKTP, TLD, and TK performed the experiments. TKTP, TLD, KT, and TK analyzed and interpreted the data. TKTP, TLD, and TK drafted the manuscript. KT revised the manuscript. All authors read and approved the final version of the manuscript.

Abstract

Surface stiffness is a unique indicator of various cellular states and events and needs to be tightly controlled. α-Mangostin, a natural compound with numerous bioactivities, reduces the mechanical stiffness of various cells; however, the mechanism by which it affects the actin cytoskeleton remains unclear. We aimed to elucidate the mechanism underlying α-mangostin activity on the surface stiffness of leukocytes. We treated spherical non-adherent myelomonocytic KG-1 cells with α-mangostin; it clearly reduced their surface stiffness and disrupted their microvilli. The α-mangostin-induced reduction in surface stiffness was inhibited by calyculin A, a protein phosphatase inhibitor. α-Mangostin also induced KG-1 cell adhesion to a fibronectin-coated surface. In KG-1 cells, a decrease in surface stiffness and the induction of cell adhesion are largely attributed to the dephosphorylation of ezrin/radixin/moesin proteins (ERMs); α-mangostin reduced the levels of phosphorylated ERMs. It further increased protein kinase C (PKC) activity. α-Mangostin-induced KG-1 cell adhesion and cell surface softness were inhibited by the PKC inhibitor GF109203X. The results of the present study suggest that α-mangostin decreases stiffness and induces adhesion of KG-1 cells via PKC activation and ERM dephosphorylation.

Keywords

alpha-mangostin, leukocytes, mechanical stiffness, ERM, PKC

Introduction

α-Mangostin is the most emblematic xanthone compound found in the pericarp of mangosteen fruit (Garcinia mangostana). Many studies have proven its extensive biological activities and pharmacological properties including antineoplastic, antioxidant [1], anti-inflammatory [2], and anti-carcinogenicity [3]. Previous research indicated that α-mangostin inhibits the subsistence of lung cancer cells and inhibits their migration and invasion [4]. A recent study found that α-mangostin was able to reduce the mechanical stiffness of various cells, including human myeloblasts KG-1 cells [5].

Surface stiffness is a unique indicator for different cellular states and events, therefore it needs to be tightly controlled [6,7]. For example, cortical stiffness changes during mitotic cell rounding [6,8], retinal epithelium stiffness changes during optic-cup morphogenesis [9,10], and leukocyte surface rigidity decreases when the cells adhere in response to external stimuli [11,12]. These features and alterations are primarily attributed to the actin cytoskeleton, which is the major mechanical structure of cells [13–16]. As α-mangostin reduces the surface stiffness of various cells [5], it probably affects the architecture of the actin cytoskeleton, via which it can affect most of the animal cells. However, clarification regarding the mechanism by which α-mangostin affects the actin cytoskeleton is still lacking. This study elucidates the mechanism by examining the effects of α-mangostin on the actin cytoskeleton layer located underneath the plasma membrane of leukocytes.

Leukocytes are non-adherent, spherical-shaped cells with microvilli on their surfaces. Microvilli are actin-rich protrusions that are localized at the non-adherent surface of leukocytes [17]. The actin cytoskeleton in leukocytes is mainly cortical actin with microvilli, and it mechanically supports the cells [11,12]. Leukocytes have relatively high surface stiffness [5]; it probably helps the cells to maintain a spherical shape and withstand the rigors of circulation. However, in some situations, such as in response to external stimuli, leukocytes deform their cell shape and transfer to adhesion with other cells or substratum[18–20], leading to a decrease in their surface rigidity [12].

The decrease in stiffness associated with cell adhesion, in leukocytes, is closely linked to ezrin/radixin/moesin (ERMs) [12]. These are cytoplasmic proteins consisting of an actin-binding domain at the C-terminus and a membrane protein-binding FERM

domain at the N-terminus, that link cortical actin to the plasma membrane [17,21]. These bonds are maintained by ERM activation (phosphorylation at a specific C-terminal threonine residue). Phosphorylated ERMs are found on non-adherent surfaces, such as the leukocyte surface and the brush border of intestinal epithelial cells [17,21]. Moesin-T558D expression, a phospho-mimetic Moesin mutant, inhibits both cell-substratum and cell-cell adhesion in HEK293T cells, that indicates the adhesion-inhibitory function of phosphorylated ERM [22,23]. Conversely, dephosphorylation of ERMs unlinks the cortical actin and the plasma membrane, which induces the microvilli to collapse and decreases cell surface rigidity [11,12,24]. Protein kinase C (PKC) activation is a key event in the upstream signaling cascade of the ERM dephosphorylation in leukocytes [11]. PKC inhibitors inhibit ERM dephosphorylation and cell adhesion induced by external stimuli or phorbol 12-myristate 13-acetate (PMA) in KG-1 cells and T lymphocytes [11]. In addition, protein phosphatase 1/2A also contributes to the PMA-induced reduction of phosphorylated ERM and adhesion in KG-1 cells because the protein phosphatase inhibitor calyculin A inhibits them [11].

This study examines the mechanism by which α-mangostin reduces the surface stiffness of KG-1 cells. Here, ERM dephosphorylation was shown to be the key event, and other related phenomena, including cell adhesion, were observed by treatment with α-mangostin. In addition, these events were inhibited by the PKC inhibitor GF109203X.

Materials and methods

Materials

Human leukemia myeloblast KG-1 cells and human lymphoma U937 DE-4 cells were obtained from Riken BioResource Research Center (Ibaraki, Japan). Rhodamine-labeled phalloidin, α-mangostin, cytochalasin D, and calyculin A were purchased from FUJIFILM Wako Pure Chemical (Osaka, Japan). GF109203X was obtained from Cayman Chemical (Ann Arbor, MI). The cell anchoring molecule, SUNBRIGHT OE-020CS, was purchased from NOF Corporation (Tokyo, Japan). The AFM probe (SN-AF01S-NT; spring constant: approximately 0.06 N/m) was purchased from Hitachi High-Tech (Tokyo, Japan). Fetal bovine serum (FBS) and Pierce BCA Protein Assay Reagent were purchased from Thermo Fischer Scientific (Tokyo, Japan). Antibiotics,

PMA, RPMI1640 medium, and monoclonal anti-β-actin antibody were purchased from Sigma-Aldrich (St. Louis, MO). Fibronectin from bovine serum was purchased from Life Laboratory Company (Yamagata, Japan). Glass-based culture dishes were purchased from Matsunami Glass (Osaka, Japan). A microflow channel (μ-slide VI 0.4) was purchased from ibidi (Grafelfing, Germany). Protease inhibitor cocktail and phosphatase inhibitor cocktail were purchased from Roche (Basel, Switzerland). Monoclonal anti-phospho-ERM antibody was purchased from Cell Signaling Technology (Danvers, MA). PKC Kinase Activity Assay Kit was purchased from abcam (Cambridge, UK). EZWestBlue W was purchased from ATTO (Tokyo, Japan). Other reagents were purchased from Sigma-Aldrich, FUJIFILM Wako Pure Chemical, or Thermo Fischer Scientific.

Preparation of cell anchoring dishes

The culture dishes were coated with SUNBRIGHT OE-020CS as described previously [5,25]. These dishes were briefly coated with BSA followed by coating with 1 mM SUNBRIGHT OE-020CS. The floating cells are caught at one end of the molecule in coated dishes [26].

Cell culture

The KG-1 cells and U937 DE-4 cells were cultured in RPMI1640 medium containing 10% FBS and antibiotics (100 units/mL penicillin G and 100 μg/mL streptomycin sulfate) in a humidified atmosphere of 95% air and 5% CO_2 at 37 °C.

Atomic force microscopy measurements

The cell stiffness was measured using atomic force microscopy (AFM) (Nanowizard III; JPK Instruments AG, Berlin, Germany) at room temperature. The KG-1 cells and U937 DE-4 cells were first plated on cell anchoring dishes for 1.5 h in serum-free medium, next washed with PBS to remove unattached cells, and then cultured for 6 h in a complete culture medium containing α-mangostin. The probe was indented at 25 different points within 1 μm × 1 μm of cell top with a loading force of up to 0.5 nN and velocity of 5 μm/s. The Young's modulus of the cell surface was determined as

described before [8,12]. More than 20 cells and 500 force-distance curves were analyzed for each condition.

Actin filament staining

The KG-1 cells were plated on cell-anchoring glass base dishes for 1.5 h in a serum-free medium, next washed with PBS to remove floating cells, and then cultured in a complete culture medium containing either 10 μM α-mangostin for 6 h or 2 μg/mL cytochalasin D for 1.5 h. The cells were then fixed with 4% paraformaldehyde, permeabilized with 0.3% TritonX-100, and then stained with rhodamine-labeled phalloidin for actin filaments. Specimens were observed using confocal laser scanning microscopy (CLSM) (Nikon C2; Nikon, Tokyo, Japan).

Adherent assay

The microflow channels were incubated for 1 h at room temperature with PBS containing 50 μg/mL fibronectin, then washed with the complete medium. The KG-1 cells were suspended in complete medium containing α-mangostin (1×10^6 cells/mL) and cultured in fibronectin-coated channels for 3 h. The U937 DE-4 cells were suspended in serum-free medium containing α-mangostin (1.6×10^6 cells/mL) and cultured in fibronectin-coated channels for 1 h. To count the cells, the slides were washed thrice with the medium to remove unattached cells, and the specimens were photographed using a phase-contrast microscope. The data were analyzed using ImageJ software (NIH, Bethesda, MD).

Immunoblotting

KG-1 cells were incubated for 30 min in the culture medium with PMA (100 nM), α-mangostin (10 μM), or α-mangostin (10 μM) and calyculin A (10 nM). Cellular lysates were prepared in RIPA buffer (1 mM Tris-HCl, pH 8.8; 150 mM NaCl; 1% SDS; and 1 mM EDTA) with protease inhibitor cocktail and phosphatase inhibitor cocktail. Protein concentration was determined using Pierce BCA Protein Assay Reagent according to the manufacturer's instructions. An equal amount of each lysate was separated by SDS-PAGE and transferred onto a PVDF membrane. The membrane was blocked with 5%

BSA and incubated with primary antibodies followed by HRP-conjugated secondary antibodies. The complex with the HRP-linked secondary antibody was detected using EzWestBlue W.

PKC activity assay

The KG-1 cells were incubated for 30 min in the culture medium with PMA (100 nM), α-mangostin (10 μM), or α-mangostin (10 μM) and calyculin A (10 nM). Cellular lysates were prepared in lysis buffer (25 mM HEPES, pH7.6; 250 mM NaCl; 1% Triton X-100; 1 mM DTT) with protease inhibitor cocktail and phosphatase inhibitor cocktail. Protein concentration was determined using Pierce BCA Protein Assay Reagent according to the manufacturer's instructions. An equal amount of each lysate was analyzed using PKC Kinase Activity Assay Kit according to the manufacturer's instructions.

Statistical analysis

The values obtained for each group were compared using one-way analysis of variance and Dunnett's pairwise comparison test. Values of p less than 0.05 were considered statistically significant.

Results

α-Mangostin reduces the mechanical stiffness of KG-1 cells

Firstly, we compared the magnitude of the surface softening effect of α-mangostin to that of actin-depolymerizing reagent cytochalasin D in KG-1 cells (Fig. 1). KG-1 cells are non-adherent cells derived from acute myelogenous leukemia with microvilli on their surface [27]. Using KG-1 cells, we have been studying the relationship between cell surface stiffness and physiological changes in leukocytes [11,12]. Upon treatment with cytochalasin D, the surface stiffness of KG-1 cells was reduced from 2.0 kPa to 0.51 kPa (Fig. 1). It showed that the mechanical strength of KG-1 cells is attributable to the actin cytoskeleton. Upon treatment with more than 10 μM α-mangostin, the Young's modulus decreased to a similar value as that of cytochalasin D treatment (Fig. 1). Thus, α-mangostin attenuates the mechanical strength of KG-1 cells, similar to cytochalasin D.

The architecture of F-actin was observed using CLSM in KG-1 cells treated with α-mangostin (Fig. 2). In untreated cells, the cell surface was covered by F-actin with short microvilli (Fig. 2). Upon treatment with cytochalasin D, the cortical actin of KG-1 cells was mostly destroyed, and F-actin aggregates were clearly observed (Fig. 2). On the other hand, the changes caused by α-mangostin differed from those caused by cytochalasin D. Two main visible alterations were observed: loss of microvilli and blebbing formation (Fig. 2). Blebbing typically occurs when the plasma membrane detaches from the cortical actin cytoskeleton [28]. The formation of microvilli is regulated by ERMs [27,29]. Cytochalasin D de-polymerizes the actin filaments whereas α-mangostin probably loosens the linkage between the plasma membrane and cortical actin caused mainly by the involvement of ERMs.

Calyculin A inhibits the α-mangostin-reduced KG-1 cell stiffness

Calyculin A, a powerful inhibitor of protein phosphatase 1/2A, diminishes ERM-dephosphorylation in KG-1 cells in response to stimuli [11,22]. To further analyze the difference between α-mangostin and cytochalasin D, we examined whether the reduction of stiffness in α-mangostin or cytochalasin D treated KG-1 cells was affected by calyculin A (Fig. 3). The KG-1 cells were exposed to 10 μM of α-mangostin or 2 μg/mL of cytochalasin D in the presence of various concentrations of calyculin A (0.3, 1.0, or 3.0 nM). The reduction in Young's modulus induced by α-mangostin was inhibited by calyculin A in a dose-dependent manner (Fig. 3). In particular, the addition of 3.0 nM calyculin A abrogated the effect of α-mangostin. However, the decrease in cell stiffness induced by cytochalasin D did not change significantly in presence of calyculin A (Fig. 3). It is presumed that α-mangostin affects cellular stiffness via dephosphorylation of ERMs.

α-Mangostin induces KG-1 cell adhesion to fibronectin substrate

When ERMs of KG-1 cells are dephosphorylated by PMA or staurosporine, cell adhesion is activated [11,12]. We then examined whether α-mangostin induced cell adhesion to the plasma fibronectin substrate using a microflow channel (Fig. 4). The number of adhered cells in the control and PMA-treated groups were approximately 120

and 430 cells/mm^2, respectively (Fig. 4). Upon treating with α-mangostin, the number of adhered cells increased in a dose-dependent manner. Thus, α-mangostin induced KG-1 cell adhesion, similar to the reagents inducing dephosphorylation of ERMs.

Then, we examined whether calyculin A inhibited the effect of α-mangostin-induced cell adhesion (Fig. 5). The KG-1 cells were co-treated with α-mangostin and calyculin A for 3 h, and the adherent cells were calculated. The amount of adherent KG-1 cells induced by α-mangostin was inhibited by calyculin A (Fig. 5). Thus, it inferred that the same mechanism regulated both the α-mangostin-induced cell adhesion and cell stiffness softening.

Similar results were obtained with U937 DE-4 cells, another human monocytic cell line; α-mangostin decreased cell surface stiffness and induced cell adhesion (Supplementary Figs. S1 and S2).

α-Mangostin induces ERM dephosphorylation in KG-1 cells

A decrease in cell surface stiffness, disruption of microvilli, and induction of cell adhesion in KG-1 cells are all associated with a decrease in phosphorylated ERMs [11,12,22,24]. Therefore, we determined the phosphorylation status of ERMs following treatment with α-mangostin. We detected phosphorylated ERMs in the untreated cells; after treatment with PMA for 30 min, the level of phosphorylated ERMs decreased (Fig. 6). Similarly, the level of phosphorylated ERMs in the cells treated with α-mangostin decreased (Fig. 6). Furthermore, the dephosphorylation of ERMs caused by α-mangostin was inhibited by calyculin A (Fig. 6). Thus, α-mangostin induced the dephosphorylation of ERMs.

α-Mangostin-induced cell adhesion and reduced cell stiffness are caused by increasing PKC activity

PKC contributes significantly to leukocyte adhesion in an ERM-dependent pathway [11]. Therefore, we investigated the PKC activity of KG-1 cells treated with α-mangostin. The PKC activity of the cells increased following treatment with α-mangostin (Fig. 7). This increase in activity was maintained even during co-treatment with calyculin A (Fig. 7).

Thus, α-mangostin increased PKC activity in the KG-1 cells, and this occurred upstream of ERM dephosphorylation.

We attempted to confirm whether the PKC inhibitor GF109203X could inhibit the effect of α-mangostin in KG-1 cells. We observed the architecture of F-actin in KG-1 cells that had been co-treated with α-mangostin and GF109203X; cortical actin and short microvilli structures were clearly visible (Supplementary Fig. S3). We then investigated the inhibitory effect of GF109203X on α-mangostin-induced cell adhesion and reduced cell stiffness. The KG-1 cells were co-treated with α-mangostin and GF109203X for 3 h, and the number of adherent cells was determined. α-Mangostin-induced cell adhesion was suppressed by GF109203X in a dose-dependent manner (Fig. 8). We also investigated the surface stiffness of KG-1 cells co-treated with α-mangostin and GF109203X. The α-mangostin-induced reduction in Young's modulus was inhibited by GF109203X (Fig. 9). Therefore, we confirmed that α-mangostin induced KG-1 cell adhesion and reduced cell surface stiffness via PKC activation.

Discussion

In the present study, we investigated the mechanism by which α-mangostin reduces the mechanical stiffness of KG-1 cells. The mechanism was clearly different from that of the actin-depolymerizing drug cytochalasin D, and the decrease in surface stiffness was related to ERMs. In KG-1 cells, α-mangostin induced ERM dephosphorylation, cell adhesion to the fibronectin surface, and PKC activation. The effects of α-mangostin on cell adhesion and surface stiffness were diminished by the PKC inhibitor GF109203X. α-Mangostin induces cell adhesion and reduces the mechanical stiffness of KG-1 cells through the PKC activation-ERM dephosphorylation pathway, similar to that induced by PMA [11].

As with cytochalasin D, α-mangostin significantly reduced the surface stiffness of KG-1 cells (Fig. 1). However, the architecture of the cortical actin that had been treated with α-mangostin appeared different from that had been treated with cytochalasin D (Fig. 2). α-Mangostin induced microvilli collapse and blebbing in cortical actin (Fig. 2). Furthermore, the mechanism of surface softening by α-mangostin was also different from that by cytochalasin D. Calyculin A inhibited α-mangostin-induced softening (Fig.

3), which indicated that α-mangostin effects through the process of protein dephosphorylation. Therefore, instead of directly affecting actin depolymerization, α-mangostin targets actin cytoskeletal microstructures via protein dephosphorylation and attenuates mechanical stiffness.

How does α-mangostin regulate the microstructure of cortical actin in KG-1 cells? α-Mangostin reduces the level of phosphorylated ERMs (Fig. 6), which link transmembrane proteins to the cortical actin. A decrease in phosphorylated ERMs undoes the link, collapses the microvilli, and reduces surface stiffness [11,12,17,21]. These factors contribute to cell adhesion in leukocytes [11,12,17,21]. In the present study, we also found that α-mangostin induced KG-1 cell adhesion (Fig. 4). Cell adhesion and ERM dephosphorylation were inhibited on treatment with calyculin A (Figs. 5, 6), which inhibits PMA- or staurosporine-induced ERM dephosphorylation [11,22]. Therefore, it is reasonable to assume that α-mangostin regulates the microstructure of cortical actin by inducing the dephosphorylation of ERMs.

The activation of PKC is critical for leukocyte adhesion induced by external stimuli via ERM dephosphorylation [11]. In the present study, we discovered that α-mangostin increased PKC activity (Fig. 7). The PKC inhibitor GF109203X inhibited α-mangostin-induced cell adhesion and cell softening (Figs. 8,9). Thus, α-mangostin affects KG-1 cells by activating PKC. Although α-mangostin was reported to activate the expression of PKC-δ in retinal cells [30], it is unclear at the present time which subtype of PKC is targeted by α-mangostin in leukocytes. Calyculin A inhibited α-mangostin-induced KG-1 cell adhesion and softening (Figs 3,5) but did not inhibit the increase in PKC activity (Fig. 7). Therefore, protein phosphatase 1/2A is potentially responsible for the signal between PKC activation and ERM dephosphorylation. The proposed signaling scheme is shown in Fig. 10.

Cell adhesion plays an important role during the early stages of leukocyte activation [18–20]. The adhesion of leukocytes to a substrate is necessary for the extravasation step, and adhesion to antigen-presenting cells is essential for immunological synapse formation [31]. To achieve these goals, the microvillus structure must be locally disassembled at the interaction site, and anti-adhesion molecules (CD34 and CD43) must be moved away; both processes require the dephosphorylation of

ERMs [32–34]. Soft leukocytes are more advantageous for cell adhesion because they can expand the contact area [12,35]. In 3A9 hybridoma cells softened by PMA treatment, the force required for detachment from an ICAM-1-immobilized surface is high [36]. In fact, ERM dephosphorylation stimuli decrease surface stiffness and induce cell adhesion in KG-1 cells [11,12]. However, no obvious alteration in the surface expression of adhesion molecule α4β1 integrin or anti-adhesion molecule CD34 has been observed following PMA treatment [11]. Thus, without accompanying alteration of integrin expression, ERM dephosphorylation sufficiently induces cell adhesion in KG-1 cells, and α-mangostin induces ERM dephosphorylation, resulting in cell adhesion (Figs. 4,6 and Supplementary Figs. S1,S2).

Is the mechanism of cell surface softening caused by α-mangostin is the same in other cells as in KG-1 cells? α-Mangostin reduces the rigidity of KG-1 cells and various cells, including normal human fibroblasts and cancer cells [4,5]. The sensitivity of α-mangostin varies in different cell types, and it is possible that the microvillus structures are the target of α-mangostin [5]. Phosphorylated ERMs are enriched in microvilli and control their structure [17,27,37]. Thus, the effect of α-mangostin on microvillus-rich cells is most likely caused by the inactivation of ERMs. How does α-mangostin work on cells without microvillus structures, such as fibroblasts? It is reported that α-mangostin inhibits myosin light-chain kinase [38], and reduces Ca^{2+} elevation by suppressing Ca^{2+} influx [39], these can negatively modulate actin cytoskeleton. Thus, the cell softening effects of α-mangostin on fibroblasts and other cells may be achieved by these actions of α-mangostin.

In cancer cells, ezrin is linked with cancer progression [40]; and its suppression resulted in the inhibition of metastasis in mouse osteosarcoma cell lines, prostatic intraepithelial neoplasia, and primary cutaneous melanoma [41–43]. Thus, the inactivation and dephosphorylation of ERMs in cancer cells influence both cell rigidity and cancer progression. The anti-metastatic properties of α-mangostin have been reported in many carcinoma cells [4,44–46]. The inhibitory effect of α-mangostin on MMP-2, MMP-9, and NF-κB prevents metastatic activity [44,45,47]. The ERM dephosphorylation effects of α-mangostin may also contribute to its anti-metastatic properties.

Although there have been many studies on the various biological activities of α-mangostin, its effect on the actin cytoskeleton and mechanical properties of cells was unclear. α-Mangostin attenuates cortical actin by decreasing phosphorylated ERMs in leukocytes, leading to microvilli disruption and reduction of cell surface stiffness. Protein phosphatase 1/2A and PKC are involved in this process. This report is the first to elucidate the mechanism by which α-mangostin acts on the actin cytoskeleton of leukocytes.

Declarations

Founding

This work was supported by JSPS KAKENHI Grant Number JP21K04797, MEXT Promotion of Distinctive Joint Research Center Program Grant Number JPMXP0621467946, and grant for Young Scientists, Institute of Environmental Science and Technology, The University of Kitakyushu.

Conflict of Interest

The authors declare that there is no conflict of interest.

Ethics approval

This work does not involve human participants or their data. In this study, we used KG-1 cell line RRID:CVCL_0374 and U937 DE-4 cell line RRID:CVCL_8765, which obtained from RIKEN BioResource Center (Ibaraki, Japan).

Informed consent

Not applicable.

References

1. Jung H-A, Su B-N, Keller WJ, Mehta RG, Kinghorn AD. Antioxidant xanthones from the pericarp of Garcinia mangostana (Mangosteen). J Agric Food Chem.

2006;54:2077–82.
2. Zuo J, Yin Q, Wang L, Zhang W, Fan Y, Zhou Y-Y, et al. Mangosteen ethanol extract alleviated the severity of collagen-induced arthritis in rats and produced synergistic effects with methotrexate. Pharm Biol. 2018;56:455–64.
3. Akao Y, Nakagawa Y, Iinuma M, Nozawa Y. Anti-cancer effects of xanthones from pericarps of mangosteen. Int J Mol Sci. 2008;9:355–70.
4. Phan TKT, Shahbazzadeh F, Pham TTH, Kihara T. Alpha-mangostin inhibits the migration and invasion of A549 lung cancer cells. PeerJ. 2018;6:e5027.
5. Phan TKT, Shahbazzadeh F, Kihara T. Alpha-mangostin reduces mechanical stiffness of various cells. Hum Cell. 2020;33:347–55.
6. Kunda P, Pelling AE, Liu T, Baum B. Moesin controls cortical rigidity, cell rounding, and spindle morphogenesis during mitosis. Curr Biol. England; 2008;18:91–101.
7. Matzke R, Jacobson K, Radmacher M. Direct, high-resolution measurement of furrow stiffening during division of adherent cells. Nat Cell Biol. 2001;3:607–10.
8. Shimizu Y, Haghparast SMA, Kihara T, Miyake J. Cortical rigidity of round cells in mitotic phase and suspended state. Micron. 2012;43:1246–51.
9. Eiraku M, Takata N, Ishibashi H, Kawada M, Sakakura E, Okuda S, et al. Self-organizing optic-cup morphogenesis in three-dimensional culture. Nature. 2011;472:51–6.
10. Eiraku M, Adachi T, Sasai Y. Relaxation-expansion model for self-driven retinal morphogenesis: a hypothesis from the perspective of biosystems dynamics at the multi-cellular level. Bioessays. 2012;34:17–25.
11. Tachibana K, Ohnishi H, Ali Haghparast SM, Kihara T, Miyake J. Activation of PKC induces leukocyte adhesion by the dephosphorylation of ERM. Biochem Biophys Res Commun. 2020;523:177–82.
12. Kihara T, Matsumoto T, Nakahashi Y, Tachibana K. Mechanical stiffness softening and cell adhesion are coordinately regulated by ERM dephosphorylation in KG-1 cells. Hum Cell. 2021;34:1709–16.
13. Collinsworth AM, Zhang S, Kraus WE, Truskey GA. Apparent elastic modulus and hysteresis of skeletal muscle cells throughout differentiation. Am J Physiol Cell Physiol. 2002;283:C1219–27.

14. Dai J, Sheetz MP. Mechanical properties of neuronal growth cone membranes studied by tether formation with laser optical tweezers. Biophys J. 1995;68:988–96.
15. Guilak F, Erickson GR, Ting-Beall HP. The effects of osmotic stress on the viscoelastic and physical properties of articular chondrocytes. Biophys J. 2002;82:720–7.
16. Trickey WR, Vail TP, Guilak F. The role of the cytoskeleton in the viscoelastic properties of human articular chondrocytes. J Orthop Res. 2004;22:131–9.
17. Niggli V, Rossy J. Ezrin/radixin/moesin: versatile controllers of signaling molecules and of the cortical cytoskeleton. Int J Biochem Cell Biol. 2008;40:344–9.
18. Dustin ML, Springer TA. T-cell receptor cross-linking transiently stimulates adhesiveness through LFA-1. Nature. 1989;341:619–24.
19. Shimizu Y, Newman W, Gopal TV, Horgan KJ, Graber N, Beall LD, et al. Four molecular pathways of T cell adhesion to endothelial cells: roles of LFA-1, VCAM-1, and ELAM-1 and changes in pathway hierarchy under different activation conditions. J Cell Biol. 1991;113:1203–12.
20. van Kooyk Y, van de Wiel-van Kemenade P, Weder P, Kuijpers TW, Figdor CG. Enhancement of LFA-1-mediated cell adhesion by triggering through CD2 or CD3 on T lymphocytes. Nature. 1989;342:811–3.
21. Fiévet B, Louvard D, Arpin M. ERM proteins in epithelial cell organization and functions. Biochim Biophys Acta. 2007;1773:653–60.
22. Tachibana K, Haghparast SM, Miyake J. Inhibition of cell adhesion by phosphorylated Ezrin/Radixin/Moesin. Cell Adh Migr. 2015;9:502–12.
23. Tachibana K, Yamane J, Haghparast SMA, Miyake J. Sialomucin and phosphorylated-ERM are inhibitors for cadherin-mediated aggregate formation. Biochem Biophys Res Commun. 2019;520:159–65.
24. Brown MJ, Nijhara R, Hallam JA, Gignac M, Yamada KM, Erlandsen SL, et al. Chemokine stimulation of human peripheral blood T lymphocytes induces rapid dephosphorylation of ERM proteins, which facilitates loss of microvilli and polarization. Blood. 2003;102:3890–9.
25. Haghparast SMA, Kihara T, Shimizu Y, Yuba S, Miyake J. Actin-based biomechanical features of suspended normal and cancer cells. J Biosci Bioeng.

2013;116:380–5.
26. Kato K, Umezawa K, Funeriu DP, Miyake M, Miyake J, Nagamune T. Immobilized culture of nonadherent cells on an oleyl poly(ethylene glycol) ether-modified surface. Biotechniques. 2003;35:1014–21.
27. Ohnishi H, Sasaki H, Nakamura Y, Kato S, Ando K, Narimatsu H, et al. Regulation of cell shape and adhesion by CD34. Cell Adh Migr. 2013;7:426–33.
28. Charras GT, Hu C-K, Coughlin M, Mitchison TJ. Reassembly of contractile actin cortex in cell blebs. J Cell Biol. 2006;175:477–90.
29. Yamane J, Ohnishi H, Sasaki H, Narimatsu H, Ohgushi H, Tachibana K. Formation of microvilli and phosphorylation of ERM family proteins by CD43, a potent inhibitor for cell adhesion: cell detachment is a potential cue for ERM phosphorylation and organization of cell morphology. Cell Adh Migr. 2011;5:119–32.
30. Fang Y, Su T, Qiu X, Mao P, Xu Y, Hu Z, et al. Protective effect of alpha-mangostin against oxidative stress induced-retinal cell death. Sci Rep. 2016;6:21018.
31. Faure S, Salazar-Fontana LI, Semichon M, Tybulewicz VLJ, Bismuth G, Trautmann A, et al. ERM proteins regulate cytoskeleton relaxation promoting T cell–APC conjugation. Nat Immunol. 2004;5:272–9.
32. Allenspach EJ, Cullinan P, Tong J, Tang Q, Tesciuba AG, Cannon JL, et al. ERM-dependent movement of CD43 defines a novel protein complex distal to the immunological synapse. Immunity. 2001;15:739–50.
33. Delon J, Kaibuchi K, Germain RN. Exclusion of CD43 from the immunological synapse is mediated by phosphorylation-regulated relocation of the cytoskeletal adaptor moesin. Immunity. 2001;15:691–701.
34. Roumier A, Olivo-Marin JC, Arpin M, Michel F, Martin M, Mangeat P, et al. The membrane-microfilament linker ezrin is involved in the formation of the immunological synapse and in T cell activation. Immunity. 2001;15:715–28.
35. Jadhav S, Eggleton CD, Konstantopoulos K. A 3-D computational model predicts that cell deformation affects selectin-mediated leukocyte rolling. Biophys J. 2005;88:96–104.
36. Wojcikiewicz EP, Zhang X, Chen A, Moy VT. Contributions of molecular binding events and cellular compliance to the modulation of leukocyte adhesion. J Cell Sci.

2003;116:2531–9.
37. García-Ortiz A, Serrador JM. ERM proteins at the crossroad of leukocyte polarization, migration and intercellular adhesion. Int J Mol Sci. 2020;21:1502.
38. Jinsart W, Ternai B, Buddhasukh D, Polya GM. Inhibition of wheat embryo calcium-dependent protein kinase and other kinases by mangostin and gamma-mangostin. Phytochemistry. 1992;31:3711–3.
39. Itoh T, Ohguchi K, Iinuma M, Nozawa Y, Akao Y. Inhibitory effect of xanthones isolated from the pericarp of Garcinia mangostana L. on rat basophilic leukemia RBL-2H3 cell degranulation. Bioorg Med Chem. 2008;16:4500–8.
40. Clucas J, Valderrama F. ERM proteins in cancer progression. J Cell Sci. 2014;127:267–75.
41. Ilmonen S, Vaheri A, Asko-Seljavaara S, Carpen O. Ezrin in primary cutaneous melanoma. Mod Pathol. 2005;18:503–10.
42. Khanna C, Wan X, Bose S, Cassaday R, Olomu O, Mendoza A, et al. The membrane-cytoskeleton linker ezrin is necessary for osteosarcoma metastasis. Nat Med. 2004;10:182–6.
43. Pang S-T, Fang X, Valdman A, Norstedt G, Pousette A, Egevad L, et al. Expression of ezrin in prostatic intraepithelial neoplasia. Urology. 2004;63:609–12.
44. Hung SH, Shen KH, Wu CH, Liu CL, Shih YW. Alpha-mangostin suppresses PC-3 human prostate carcinoma cell metastasis by inhibiting matrix metalloproteinase-2/9 and urokinase-plasminogen expression through the JNK signaling pathway. J Agric Food Chem. 2009;57:1291–8.
45. Lee YB, Ko KC, Shi MD, Liao YC, Chiang TA, Wu PF, et al. alpha-Mangostin, a novel dietary xanthone, suppresses TPA-mediated MMP-2 and MMP-9 expressions through the ERK signaling pathway in MCF-7 human breast adenocarcinoma cells. J Food Sci. 2010;75:H13–23.
46. Shibata MA, Iinuma M, Morimoto J, Kurose H, Akamatsu K, Okuno Y, et al. alpha-Mangostin extracted from the pericarp of the mangosteen (Garcinia mangostana Linn) reduces tumor growth and lymph node metastasis in an immunocompetent xenograft model of metastatic mammary cancer carrying a p53 mutation. BMC Med. 2011;9:69.

47. Shih YW, Chien ST, Chen PS, Lee JH, Wu SH, Yin LT. Alpha-mangostin suppresses phorbol 12-myristate 13-acetate-induced MMP-2/MMP-9 expressions via alphavbeta3 integrin/FAK/ERK and NF-kappaB signaling pathway in human lung adenocarcinoma A549 cells. Cell Biochem Biophys. 2010;58:31–44.

Figure legends

Fig. 1. Young's modulus of KG-1 cells treated with α-mangostin. The cells were treated with 5, 10, or 15 μM α-mangostin for 6 h, or 2 μg/mL cytochalasin D (CD) for 1.5 h. The distribution of Young's modulus is represented by scatterplots. Each point represents the median value of 25 measuring points in each cell, and Young's modulus in each condition is represented in more than 20 independent cells. The logarithmic average value of Young's modulus (kPa) is shown at the top of each plot. *** $p < 0.001$ (Dunnett's test).

Fig. 2. Confocal laser scanning microscopy (CLSM) images of fluorescence-labeled F-actin in KG-1 cells treated with α-mangostin. KG-1 cells were treated with 10 μM α-mangostin for 6 h or 2 μg/mL cytochalasin D for 1.5 h. F-actin was stained with rhodamine-labeled phalloidin. The cells treated with α-mangostin are blebbed (arrowheads). The actin cytoskeleton of cytochalasin D-treated cells is deformed and aggregated (arrows). Bar: 20 μm.

Fig. 3. Young's modulus of KG-1 cells co-treated with α-mangostin or cytochalasin D and calyculin A. The cells were treated with 10 μM α-mangostin and 0.3, 1.0, or 3.0 nM calyculin A for 6 h, or 2 μg/mL cytochalasin D (CD) and 0.3, 1.0, 3.0 nM calyculin A for 1.5 h. The distribution of Young's modulus is represented by scatterplots. Each point represents the median value of 25 measuring points in each cell, and Young's modulus in each condition is represented in more than 20 independent cells. The logarithmic average value of Young's modulus (kPa) is shown at the top of each plot. *** $p < 0.001$ (Dunnett's test).

Fig. 4. α-Mangostin treated-KG-1 cell adhesion to a fibronectin surface in a microflow channel. **A** Phase-contrast images of KG-1 cells in the fibronectin-coated microflow channel with and without 10 μM α-mangostin for 3 h. **B** The adhered cell number of each condition. The cells were treated with 5, 10, 15 μM α-mangostin, or 50 nM of PMA for 3 h. The adhered cell number was counted from 12 different field views in each

condition. * $p < 0.05$, ** $p < 0.01$ vs. adhered cell number of control condition (Dunnett's test).

Fig. 5. Effects of calyculin A for KG-1 cell adhesion treated with α-mangostin to a fibronectin surface in a microflow channel. The cells were treated with 15 μM α-mangostin and 0.5 1.0 or 3.0 nM calyculin A (Caly-A) for 3 h. The adhered cell number was counted from 10-12 different field views in each condition. ** $p < 0.01$ vs. adhered cell number of 15 μM α-mangostin treatment condition (Dunnett's test).

Fig. 6. Immunoblot analysis of phosphorylated ERM in KG-1 cells. The KG-1 cell lysates were subjected to SDS-PAGE and immunoblotting with anti-phospho-ERM or anti-β-actin antibody. The cells were treated for 30 min with 100 nM PMA, 10 μM α-mangostin, or 10 μM α-mangostin and 10 nM calyculin A. In the immunoblot of anti-phospho-ERM, the lower molecular-weight band represents phosphorylated moesin and the band above represents phosphorylated ezrin and radixin. The bottom graph shows the normalized relative amounts of phosphorylated ERM/β-actin in each lane from independent triplicate experiments.

Fig. 7. PKC activity analysis in KG-1 cells. The cells were treated for 30 min with 10 μM α-mangostin, a combination of 10 μM α-mangostin and 10 nM calyculin A, or 100 nM PMA. ** $p < 0.01$ vs. the control (Dunnett's test).

Fig. 8. Effects of GF109203X for KG-1 cell adhesion treated with α-mangostin to a fibronectin surface in a microflow channel. The cells were treated with 15 μM α-mangostin and 0.5, 1.0, or 3.0 μM GF109203X (GF) for 3 h. The adhered cell number was counted from 10-12 different field views in each condition. ** $p < 0.01$ vs. adhered cell number of 15 μM α-mangostin treatment condition (Dunnett's test).

Fig. 9. Young's modulus of KG-1 cells co-treated with α-mangostin and GF109203X. The cells were treated with 10 μM α-mangostin for 6 h, 10 μM α-mangostin and 1.0 μM GF109203X (GF) for 6 h, or 1.0 μM GF109203X for 3 h. The distribution of Young's

modulus is represented by scatterplots. Each point represents the median value of 25 measuring points in each cell, and Young's modulus in each condition is represented in more than 20 independent cells. The logarithmic average value of Young's modulus (kPa) is shown at the top of each plot. *** $p < 0.001$ (Dunnett's test).

Fig. 10. Scheme representing α-mangostin signaling in KG-1 cells. α-Mangostin increases PKC activity and induces ERM dephosphorylation. ERM dephosphorylation is inhibited by calyculin A. The dephosphorylation of ERMs decreases surface stiffness and induces microvilli collapse, resulting in cell adhesion.

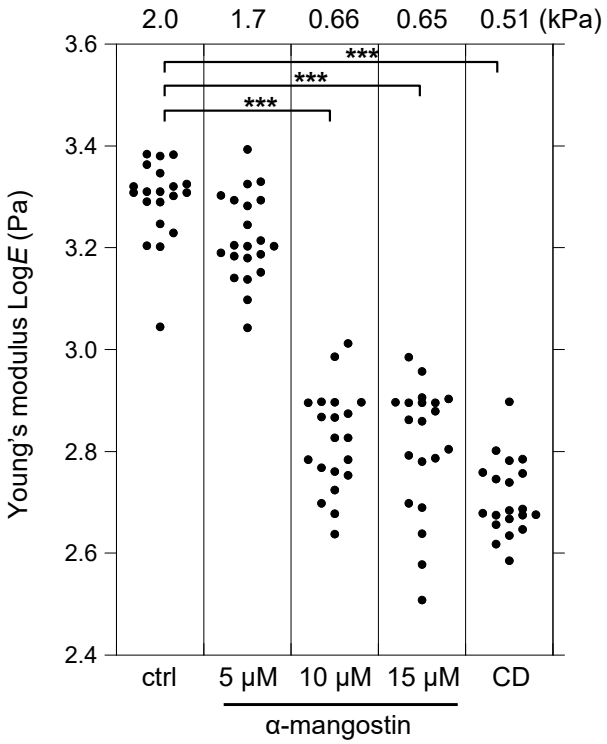

Fig. 1 Phan et al.

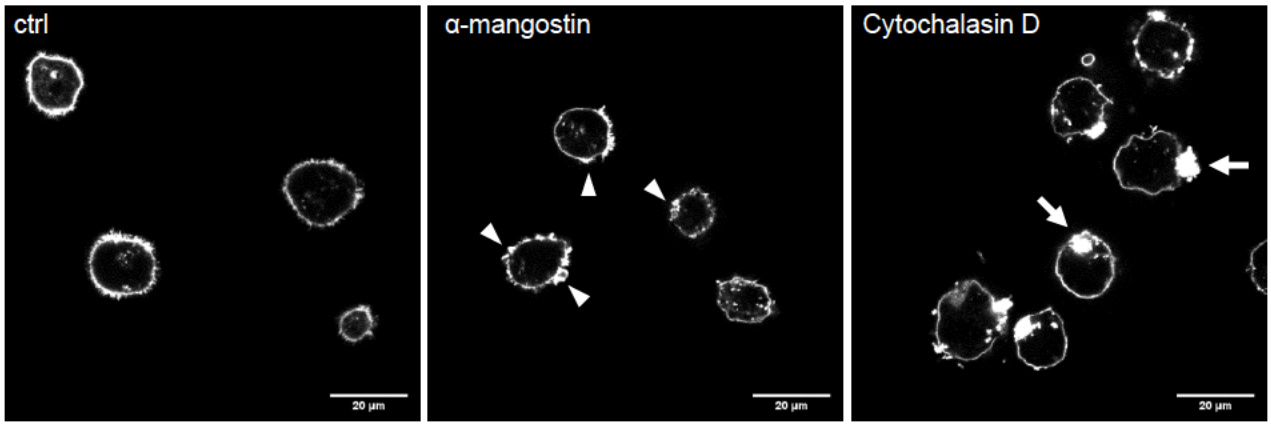

Fig. 2 Phan et al.

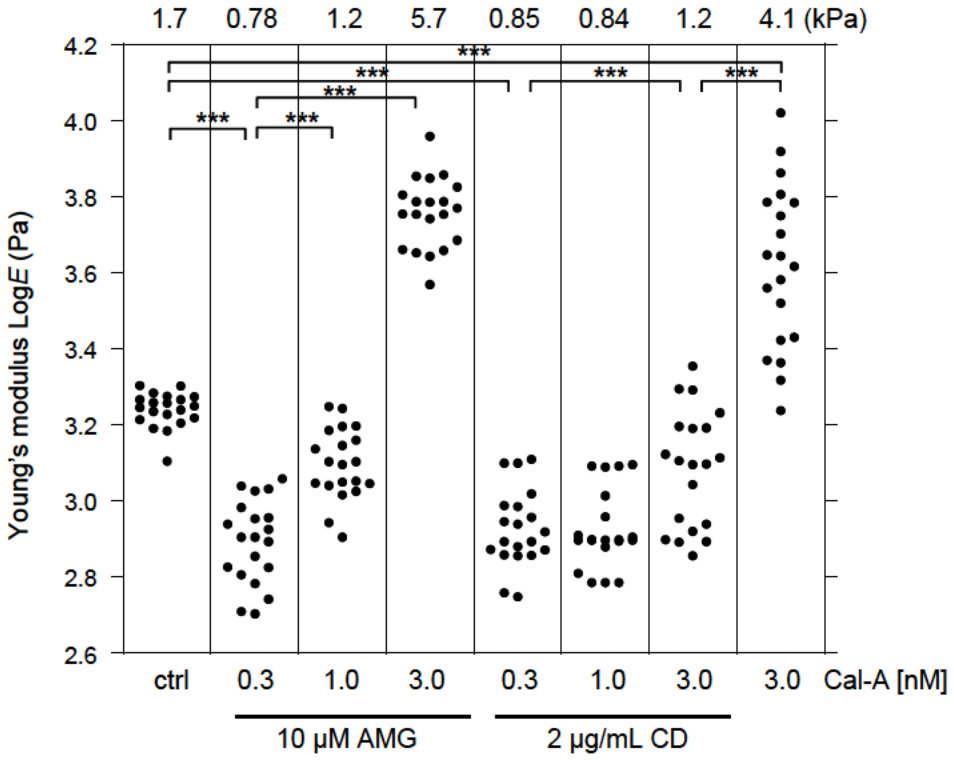

Fig. 3 Phan et al.

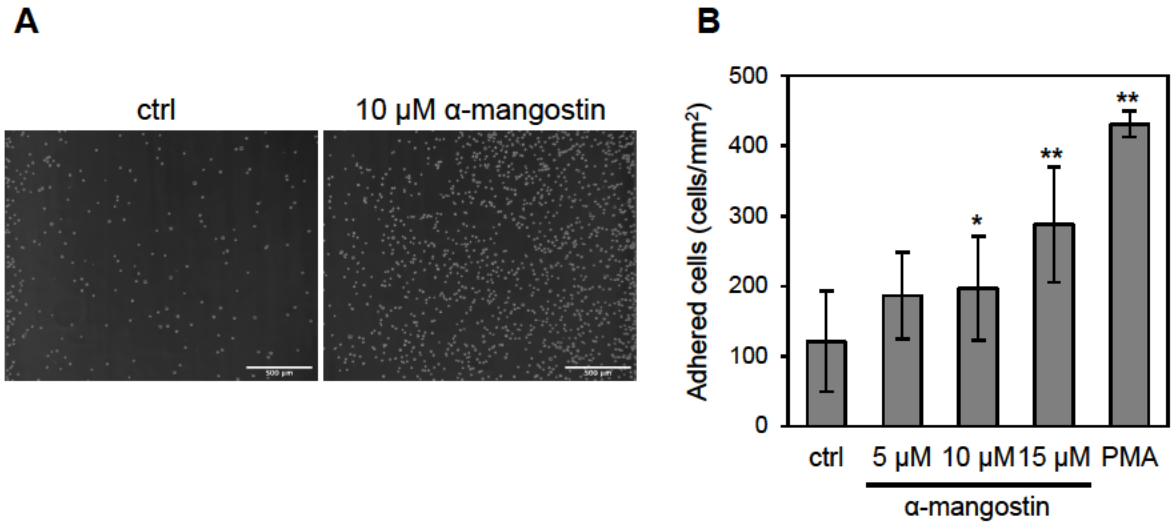

Fig. 4 Phan et al.

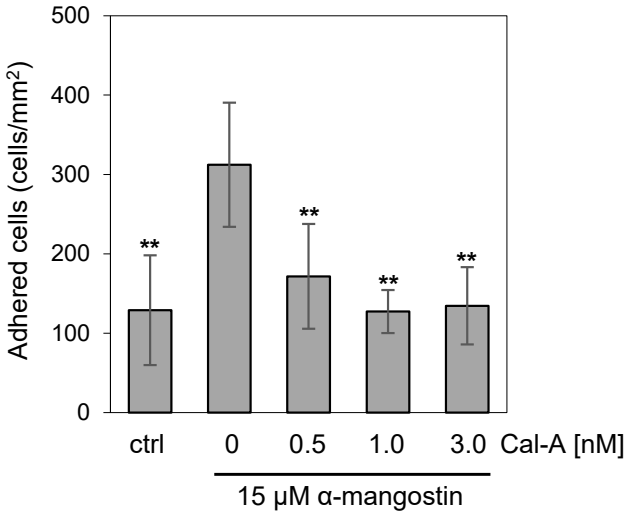

Fig. 5 Phan et al.

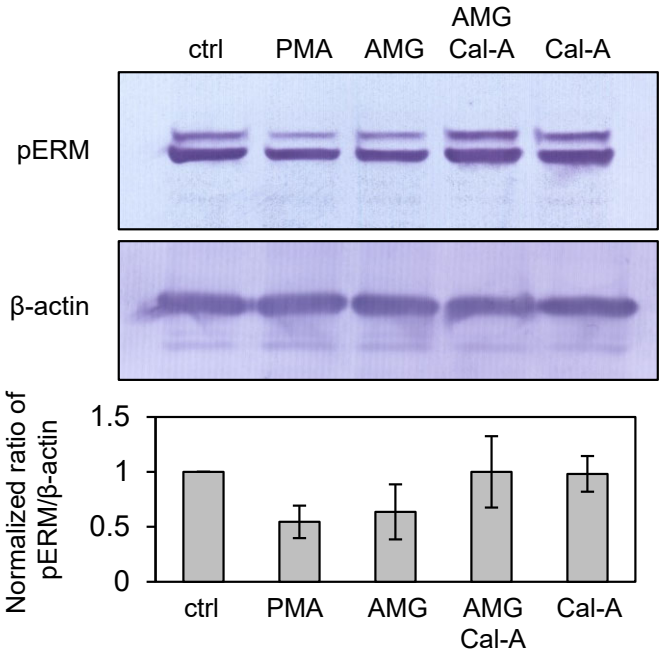

Fig. 6 Phan et al.

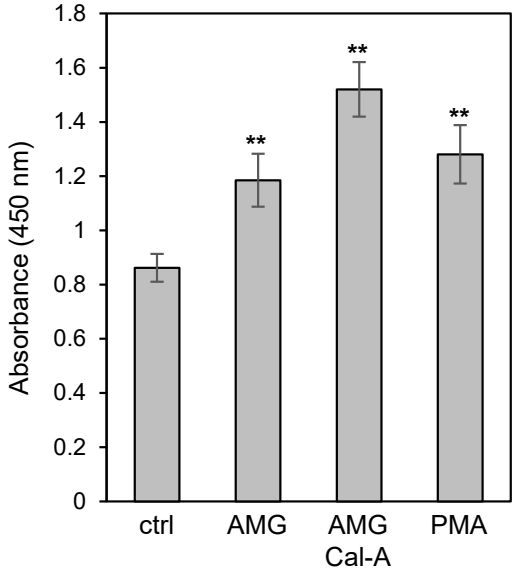

Fig. 7 Phan et al.

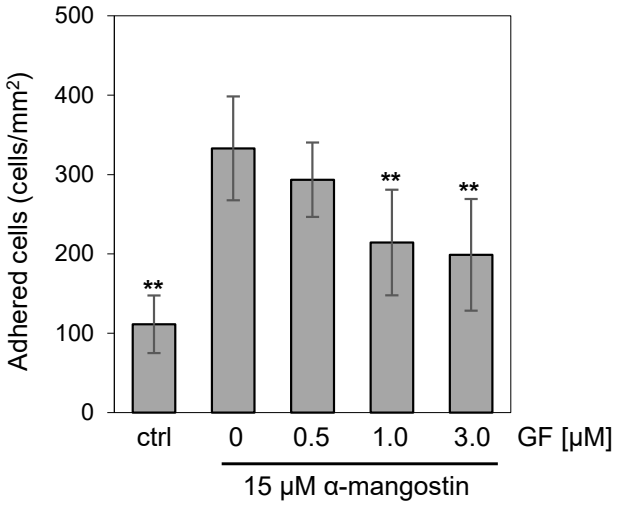

Fig. 8 Phan et al.

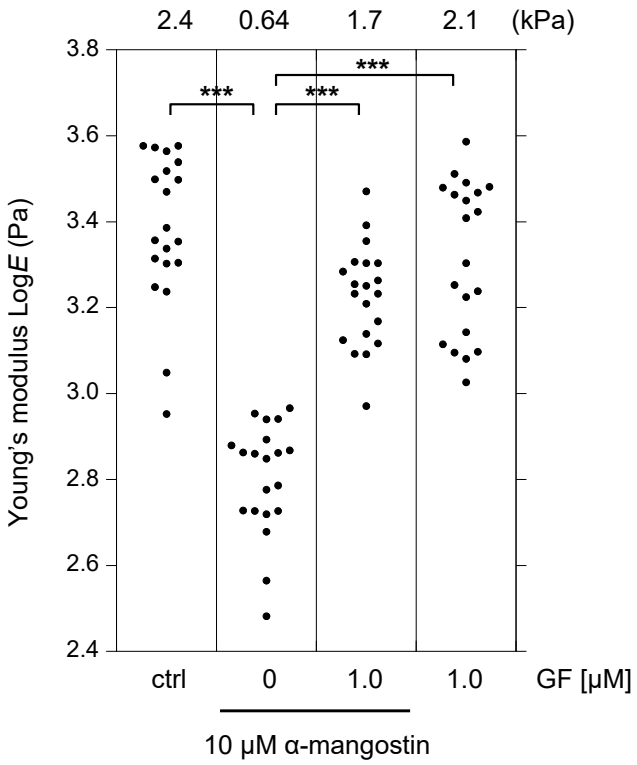

Fig. 9 Phan et al.

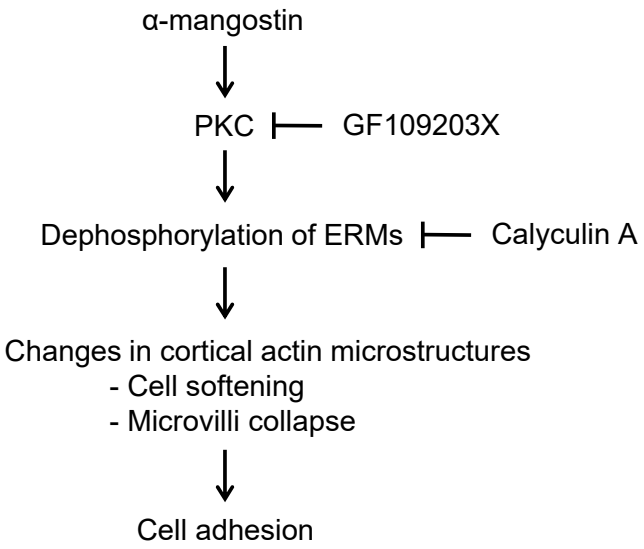

Fig. 10 Phan et al.

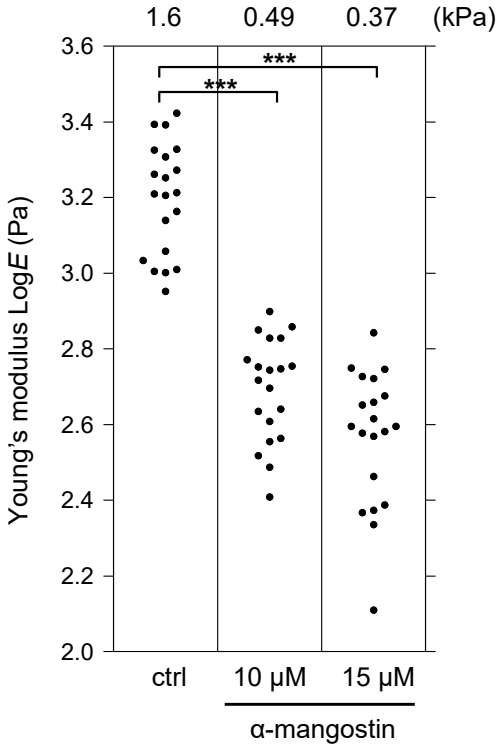

Supplementary Fig. S1. Young's modulus of α-mangostin-treated U937 DE-4 cells. The cells were treated with 10 or 15 μM α-mangostin for 6 h. The distribution of the Young's modulus is represented by scatterplots. Each point represents the median value of 25 measuring points in each cell, and the Young's modulus in each condition is represented in 20 independent cells. The logarithmic average value of the Young's modulus (kPa) is shown at the top of each plot. *** $p < 0.001$ (Dunnett's test).

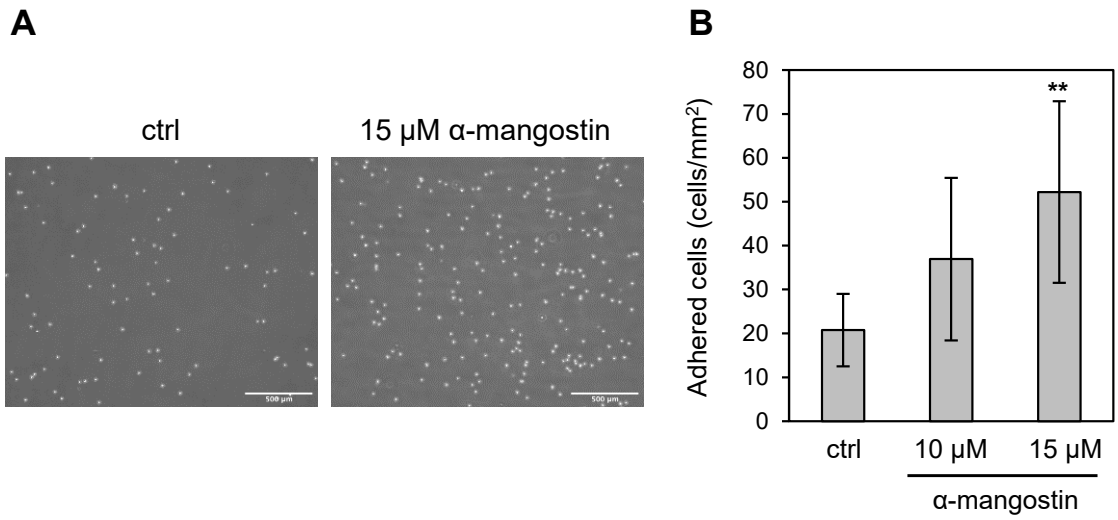

Supplementary Fig. S2. Adhesion of α-mangostin-treated U937 DE-4 cells to a fibronectin surface in a microflow channel. **A** Phase-contrast images of the adhered U937 DE-4 cells in the fibronectin-coated microflow channel with and without 15 μM α-mangostin. Bar: 500 μm. **B** The number of adhered cells associated with each condition. The cells were treated with 10 or 15 μM α-mangostin for 1 h. The adhered cells were counted in 10 different field views for each condition. ** $p < 0.01$ vs. adhered cell number of the control condition (Dunnett's test).

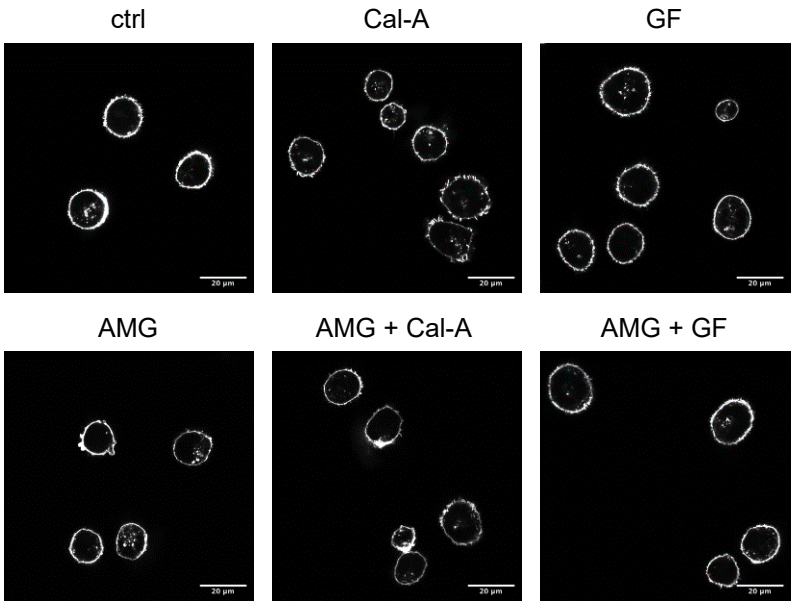

Supplementary Fig. S3. CLSM images of fluorescence-labeled F-actin in KG-1 cells treated with inhibitors. The KG-1 cells were treated with 10 μM α-mangostin, 0.2 nM calyculin A, or 1 μM GF109203X for 6 h. F-actin was stained with rhodamine-labeled phalloidin. Bar: 20 μm.